Online ISSN: 2981-0396 Print ISSN: 2981-0388

International Journal of Iron & Steel Society of Iran

Journal Homepage: https://journal.issiran.com/

Research Article

Study on Vibration of Middle Leg in The MIDREX Shaft Furnace

M. Akhondizadeh *[1], R. Bahaadini [2], O. Afsari [3]

[1] *Department of Mechanical Engineering, Sirjan University of Technology, Sirjan, Iran*
[2] *Gol-Gohar Iron & Steel Development Company, Sirjan, Iran*
[3] *Department of Mechanical Engineering, Shiraz University, Shiraz, Iran*

ARTICLE INFO

Keywords:

Middle Leg Vibration, Midrex Shaft Furnace, Material Flow, Dri.

Article history:

Received 09 March 2024
Received in revised form 07 May 2024
Accepted 26 November 2024

ABSTRACT

In the present study, the vibration of the middle leg in MIDREX shaft furnace in Gol-Gohar Iron and Steel Development company (GISDCO) has been investigated to detect the cause of vibration. For this aim, field data-collection was performed to determine the events which influence the vibration in the MIDREX shaft furnace. The effects of material flow and shocks in product-cooler and furnace were studied. The direct influenceof shocks in the furnace and product cooler on the leg vibration was rejected by detailed data analyses. However data analyses was showed that the shocks in the product cooler matched in 05 most cases with the leg vibration initiation. More precise analyses revealed that the material flow actuated the leg vibration. The shocks indirectly actuated vibration by creating a sudden blank space at the top of the product cooler which led to the opening of the leg outlet and starting the material flow. The load interaction between the flow material and the leg body behaved as an actuating force for the leg vibration.

1. Introduction

The original process was developed by the Midland-Ross Co., which later became MIDREX Technologies, Inc., a wholly owned subsidiary of Kobe Steel. MIDREX technologies also carried out various improvements to the plants that they built in multible countries. The maximum production capacity in 1984, when Kobe Steel became affiliated with MIDREX technologies, was 600 thousand tons/year. Later improvements, made by Kobe Steel in collaboration with MIDREX technologies, have dramatically increased the production capacity. In 2007, the scale reached 1.8 million tons/year. Atsushi et al. [1] studied the overview of the history of the technical developments in MIDREX processes. Hamadeh et al. [2] investigated the detailed modeling of the direct reduction of iron ore in a shaft furnace. Valipour and Saboohi [3] developed a mathematical model to investigate the reduction process of hematite in the reduction zone of the MIDREX shaft furnace as a moving bed reactor. Boechat et al. [4] studied the simulation of the mechanical degradation of iron ore pellets in a direct reduction furnace. Hosseini and Faghih Khorasani [5] performed an experimental setup and a numerical simulation that can be used to improve the efficiency of cross-flow heat exchangers in the MIDREX process. Munro and Amundson [6], Amundson [7] and, Siegmund et al. [8] used a linear function of the solid

* *Corresponding Author*
Email: m.akhondizadeh@gmail.com
Address: Department of Mechanical Engineering, Sirjan University of Technology, Sirjan, Iran
1. Assistant Professor, 2. Ph. D, 3. M. S.

DOI: http://10.22034/IJISSI.2024.2024578.1282
Published by ISSI (Iron & Steel Society of Iran)

temperature in moving bed solid–gas reactors to estimate the reaction rate. Shams and Moazeni [9] simulate the gas-based direct reduced iron (DRI) process, including reduction, transition, and cooling zones in MIDREX technology. The effect of reactor length and cooling gas flow on the metallization and the effect of cooling gas flow on the outlet temperature of the solid phase have been studied.

In the present work, the data analysis of the vibration of the middle leg is presented to describe how vibration motion starts and continues. Moreover, the data analysis results, which qualitatively describe the phenomenon, the vibration parameters are determined, and the problem is discussed by quantity. The main purpose is to determine the cause of vibration to find a solution for minimizing the vibration intensity.

2. Problem Description

A schematic of the middle leg in the shaft furnace is shown in Fig. 1. The middle leg acts as a channel for the transition of reduced iron pellets from the furnace to the product cooler. The leg is joined to the furnace and product cooler by expansion joints to accommodate the contraction-expansion effects. The leg is simply sitting on a beam structure to increase the total stiffness of leg support. The leg mass and support properties are such that the vibration under the specified actuation is possible. Non-regular leg vibration initiates during the furnace operation, lasts several seconds, and then stops. Cracks which are observed in the weldment of the leg body as illustrated in Fig. 2. are contributed to the leg vibration.

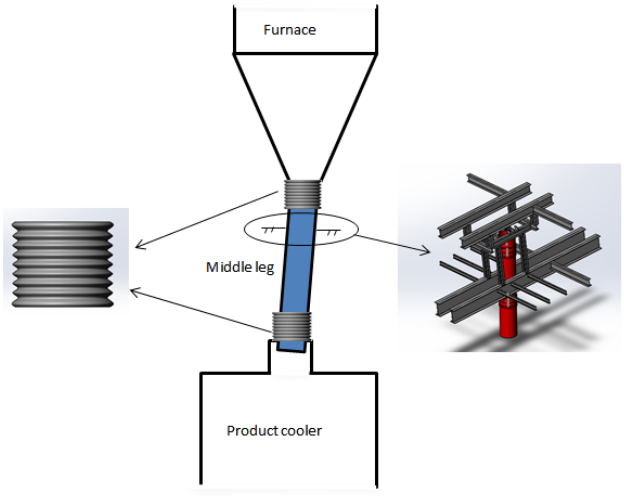

Fig. 1. Schematic of the position of the middle leg in the shaft furnace and its base structure.

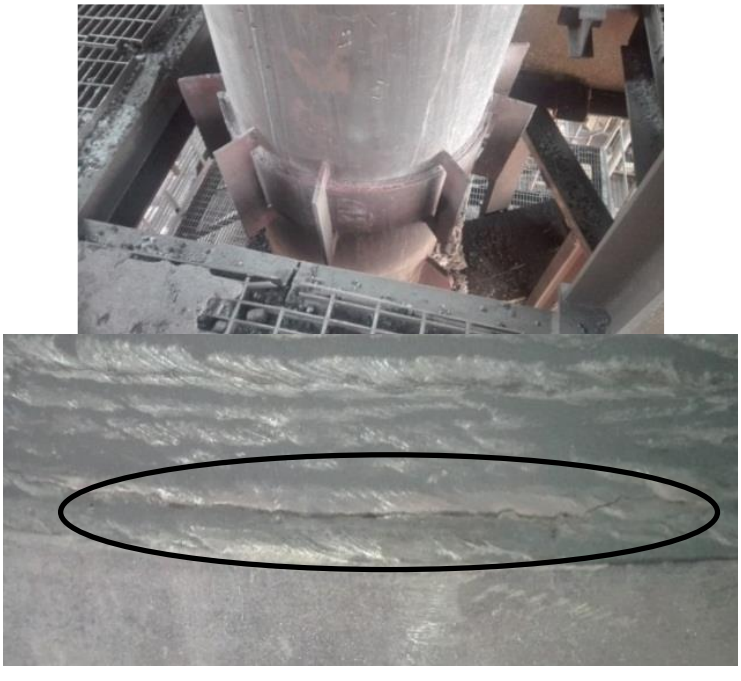

Fig. 2. Ring weldment in the leg body and a typical crack initiation in it.

3. Vibration Actuation

Data collection was performed to determine the cause of leg vibration which was actuated irregularly by the unknown source several times a minute. During the data collection, short-duration and intensive mechanical shocks were observed in the product cooler and furnace in the form of oscillating waves in their body. One of these waves which has been registered from the body of the product cooler is given in Fig. 3. This wave lasts about 2.7 seconds and the amplitude is lower than 1mm. Most of the observed waves have the identical behavior. More investigation has been done to recognize their influence on leg vibration.

Data collection was done to confirm or reject the dependence of the leg vibrations on these shocks. Accordingly, the precise time of the vibration initiation in the leg and mechanical shocks in the product cooler were registered during a specified time interval. The purpose was to determine whether the leg vibration and product cooler shocks were simultaneous or not. The registered data during 10 minutes of operation are given in Fig. 4. 22 vibration initiations in the leg and 13 shocks in the product cooler were observed during this period of time.

There are several cases in Fig. 4. where the vibration initiation in the leg and the shocks in product cooler occur at the same time. The first conclusion which comes to mind is that the shocks of the product cooler actuate the leg vibration. however, there are some highlighted cases in Fig. 4. in which vibrations in the leg do not match the shocks in the product cooler. The more data that helps us to have the better conclusion are given in Table 1.

Before presenting the final conclusions, the detailed specifications of the system of leg vibration are presented in following sections.

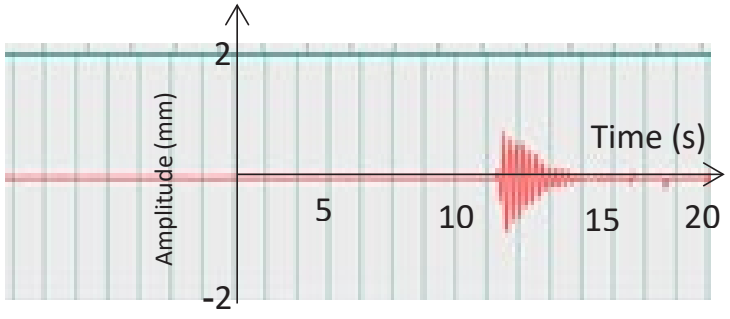

Fig. 3. A typical time domain shock in the product cooler.

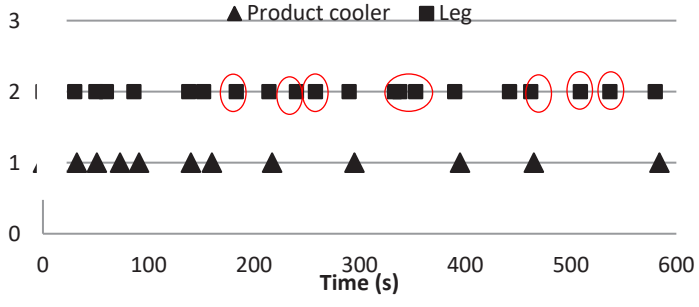

Fig. 4. Time of the vibration occurrence in leg (■) and mechanical shocks in product cooler (▲).

Table 1. Average values of time specifications of leg vibration and product cooler shocks.

Parameter	Time (s)
Leg Vibration duration	10
The average Time between two successive leg vibrations	26
The average duration of no vibration in leg	16
The average time between two successive shocks	53
Duration of shock pulse in product cooler	1.5-3

4. Leg Vibration System

A thorough observation of the system revealed that the equivalent model of the leg vibration can be considered the classic model which is illustrated in Fig. 5. This model consists of elements that constrain the leg motion in the vertical and horizontal directions. These elements are, as illustrated in Fig. 1. the expansion joints and beam structure. The values of the stiffness of these elements are in the levels that allow the leg to experience the vibration motion.

K_{y1} and K_{y2} are the stiffness of the flexible expansion joints that act in the axial direction, K_{sy} is the axial stiffness of the beam structure and C_y and C_x are the total damping of all elements in axial and lateral directions respectively. K_x and K_{sx} are the lateral stiffness of the expansion joints and beam-structure respectively. m_L is the leg mass, m_p is the influencing DRI mass and m_{es} is the equivalent mass of beam-structure. Observations and measurements showed that the vibration amplitude in the axial direction is relatively higher than the amplitude in the lateral direction which says that the main problem is the axial vibration and so the values of parameters which influence the axial vibration have been determined and are given in Table 2.

The leg is contained of DRI and its total volume is about 2.77m^3. According to the DRI density between 1.6-1.9 t/m^3 the total mass of DRI in the leg is between 4.43-5.26 tons which does not move exactly as the leg during the vibration. It is surely incorrect to consider the total DRI mass in equivalent mass. Obviously, further statements to determine the effect of material mass on leg vibration equivalent mass require a relatively comprehensive investigation of material flow behavior in the leg. There is such a problem with the evaluation of the equivalent mass of beam structure but it is estimated between 1 to 2 tons. The natural frequency of leg vibration is:

$$f = \frac{1}{2\pi}\sqrt{\frac{k_{y1}+k_{y2}+k_{sy}}{m_L+m_p+m_{es}}} = 6.35Hz \qquad \text{Eq.(1)}$$

5. Fourier Transform

The vibration measurement instruments (vibrometers) have been considerably developed in recent years.

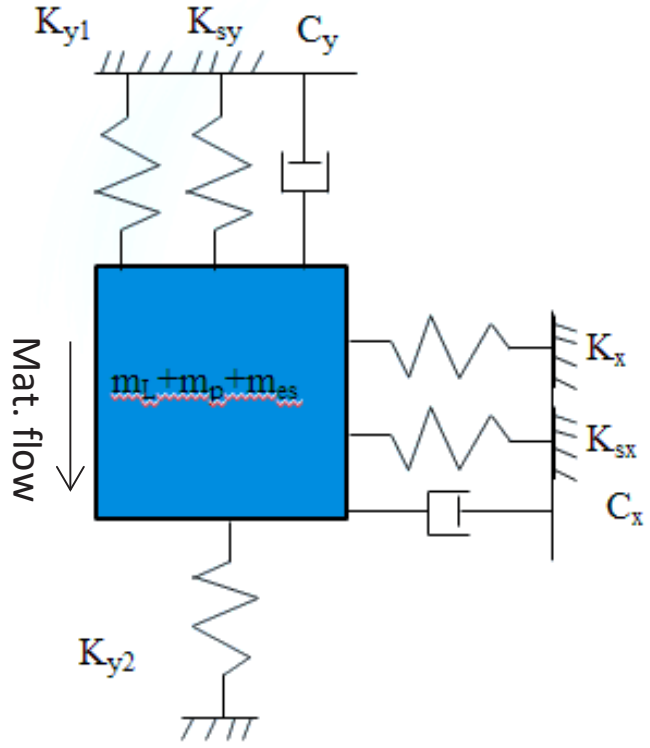

Fig. 5. The classic equivalent of the vibration system of leg.

Table 2. Parameters of the vibration system.

K_{y1}(MN/m)	K_{y2}(MN/m)	K_{sy}(MN/m)
0.86	0.68	16
m_L(ton)	m_p(ton)	m_{es}(ton)
5.12	4	2

They have noticeable abilities to measure a wide range of vibration-related parameters. A V4 vibrometer gives valuable graphs of leg vibration which one of the time domain graphs is given in Fig. 6.

Fourier transform (FT) of time domain data clarifies the vibration main frequencies. The FT of time domain data of Fig. 6. is illustrated in Fig. 7. in which the main frequency is 6.24Hz which is close to the evaluated natural frequency. It means that the leg vibration is free vibration which is actuated irregularly by an external source.

6. Source of vibration

As mentioned, it was observed during the data collection that the vibration initiation in the leg, in some cases, did not match the shock occurrence in the product cooler. Moreover, as given in Table 1. the duration of shocks in the product cooler is 1.5-2.5 seconds whereas, the average duration of leg vibration is about 10 seconds. Certainly, the inherent hysteresis damping prevents the leg vibration from lasting such long unless an external actuation applies to the leg during the vibration. After more discussions, an acceptable explanation confirmed the events related to the leg vibration.

Shock in the product cooler, which is a sudden duration vibrating motion, leads to rapid subsidence of the upper level of material in the product cooler. The material flow in leg, which was obstructed due to the material accumulation on the top of the product cooler, moves down and lasts until the obstruction occurs again. The material flow acts as an actuation for the leg vibration. There is also a description for the cases in which the leg vibration initiation does not match the shock in the product cooler. In these cases, the subsidence in the product cooler naturally happens due to the material discharge from its output, and then the material motion in the leg starts which leads to its vibration.

It is definitely accepted that the reason for the leg vibration is the flow of material through it. But the question is how does the material flow lead to the leg vibration?

There is no analytical classic model to evaluate the interaction between the flow and leg body but the discrete element method (DEM) can be helpful. Before that, to have a quantitative estimation of the actuating force, the relations of the forced vibration of a simple spring-mass system are taken under evaluation here.

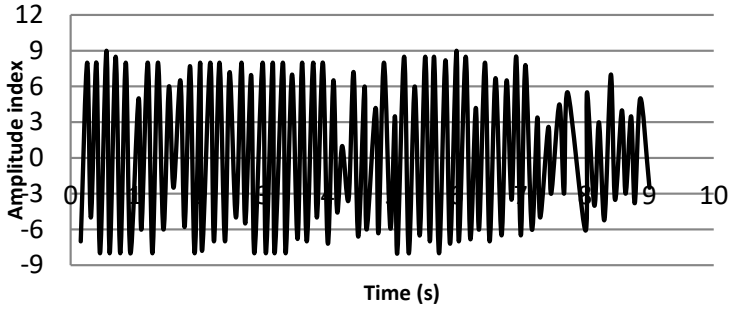

Fig. 6. The time domain of the leg vibration.

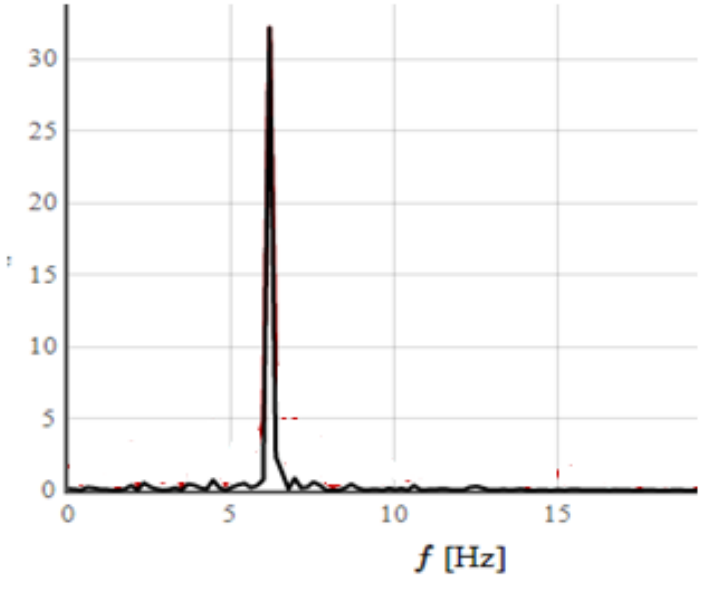

Fig. 7. Fourier transform of the leg vibration.

$$m\ddot{x} + C\dot{x} + kx = F(t) \quad \text{Eq.(2)}$$

In the present problem, F(t) is not specified as an explicit function of time so, it is replaced by the Fourier series.

$$F(t) = \sum F_{ai} cos\omega_i t + F_{bi} sin\omega_i t \quad \text{Eq.(3)}$$

By assuming the linear behavior of the vibrating system, the following summation will give the amplitude.

$$x(t) = \sum X_i cos(\omega_i t + \varphi_i) \quad \text{Eq.(4)}$$

In which

$$X_i = \frac{F_i/k}{\sqrt{(1-(\frac{\omega_i}{\omega_n})^2)^2 + 2\xi(\frac{\omega_i}{\omega_n})^2}} \quad \text{Eq.(5)}$$

$$F_i = \sqrt{F_{ai}^2 + F_{bi}^2} \quad \text{Eq.(6)}$$

The values of the system parameters including the inertia, stiffness, amplitude, damping ratio, and the resulting natural frequency should be determined for further evaluation. A discussion made on the values of the mass and stiffness is not repeated here. Since the intensity of the leg vibration was not the same in all cases a unique value was not observed for the leg vibration amplitude but it was between 2 and 3 mm in most cases. As illustrated in Fig. 8. the damping was visible in the time domain graph at the end of vibration when the actuating force vanishes due to the material flow obstruction.

The damping ratio is evaluated by the following approximate relation.

$$ln\frac{x_n}{x_m} = 2\pi\xi(m-n) \quad \text{Eq.(7)}$$

In which x_n and x_m are the amplitudes in vibration cycles n and m respectively. The summary of the system parameters is given in Table 3.

Substitution of these parameters in Eq.4 results in a relation between the applied force F_i and frequency ratio ω_i/ω_n which is a plot of it has been illustrated in fig. 9. In fact, this figure gives a tool to identify the value of F_i corresponding to the specified frequency ratio of ω_i/ω_n when a single force in the form of $F_i \sin\omega_i t$ is applied on the leg and leads to the vibration motion with 2mm amplitude. It should be noted that this is only an aid to understanding what happens here. It is clear that the nature of the present problem rejects the existence of a specified harmonic actuation force from the material flow. It is obvious that the force inserted on the leg by the material flow does not have a harmonic manner. Nevertheless, a function like Fig. 10. can be close to the real behavior of this force

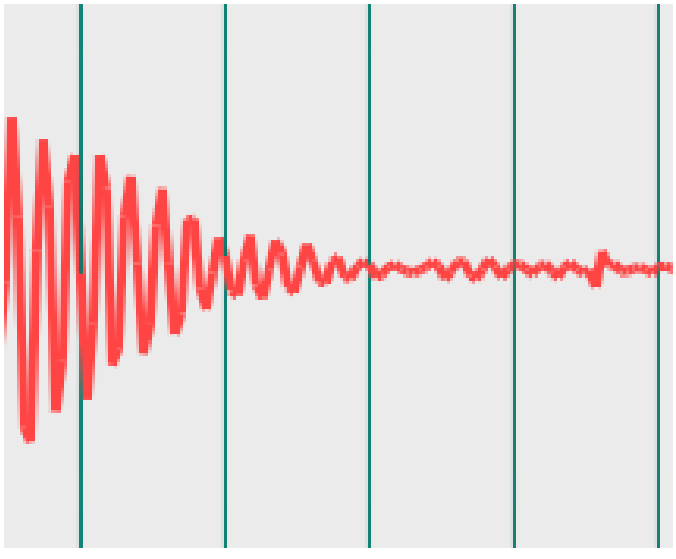

Fig. 8. Decrease of amplitude due to damping.

Table 3. Values of the vibration system parameters.

K(MN/m)	Leg mass	Structure mass	
17	5ton	1-2ton	
DRI mass	ω_n(rad/s)	X(mm)	ξ
3-5ton	37-45	2-3	0.036

which should be confirmed by more evaluations.

7. DEM Simulation of The Material Flow

A DEM simulation was programmed to have an evaluation of the material flow kinematics and the load interaction between the material and the leg body. The model includes a bin and pipe as illustrated in fig. 11. The furnace is not modeled by its geometrical details and a simple equivalent has been modeled to have a possibly short-time simulation.

The spherical-shape grains are considered as simulation material whose properties are given in Table 5.

The size distribution is given in Table 6.

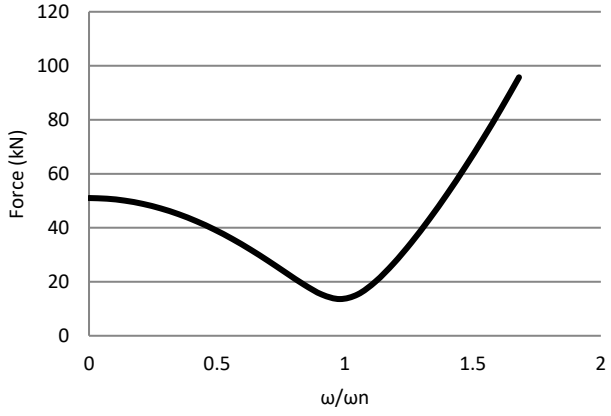

Fig. 9. The required force to have 2mm amplitude at the different frequency ratio.

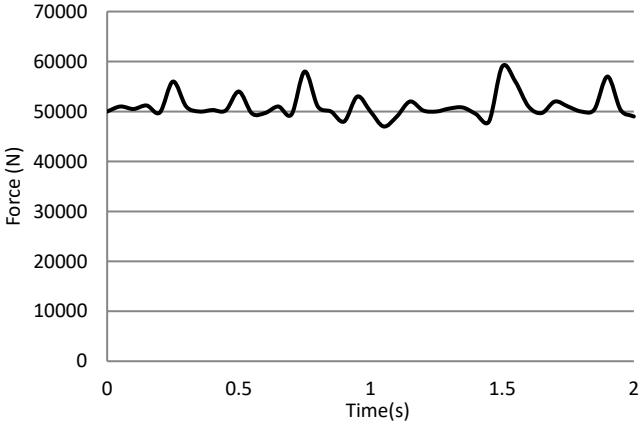

Fig. 10. Assumed load interaction between the material flow and leg body.

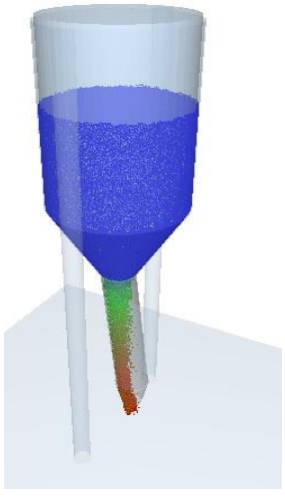

Fig. 11. 3D model for DEM Simulation.

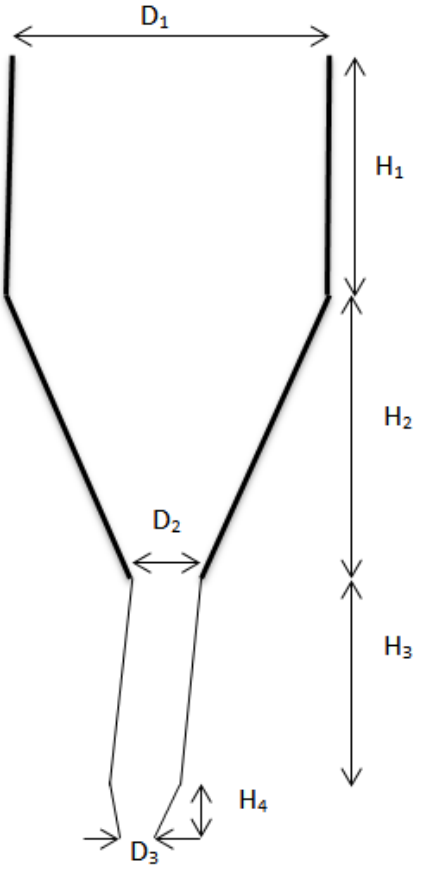

Fig. 12. Schematic model of simulation.

Table 4. Geometrical dimensions of the model.

Leg inclination	6.5 degree
H_1	2000mm
H_2	960
H_3	1700
H_4	400
D_1	1500
D_2	400
D_3	240

Table 5. Properties of simulation materials.

	Density	Shear modulus	Poisson's ratio
Pellet	3948	16000	0.25
Steel	7800	70000	0.3

Table 6. Size distribution of the material in simulation.

Size (mm)	6	8	12	16
Vol. fraction%	1.12	2.02	95.04	1.82

Table 7. Kinematic parameters of the simulation.

	e	St. Fr.	Roll. Fric.
Pellet-Pellet	0.48	0.49	0.21
Pellet-Steel	0.39	0.5	0.25

e is the coefficient of restitution. The simulation starts by opening the leg outlet while the leg and furnace are full of material. Material flows under the gravitational effect toward leg output. The simulation was let to last about 11 seconds. A typical contour of flow velocity at the 10th second is illustrated in Fig. 13.

The variation of the mass flow rate through simulation, measured at the leg outlet, has been illustrated in Fig. 14. which has irregular variations. This has the potential ability to actuate the leg vibrations.

Variation of the load interaction between the material flow and leg body through simulation is illustrated in Fig. 15. The variations like those seen in the flow rate diagram are observed which gives the conclusion that there may be a relation between load and flow rate. Obviously, limitations on material flow are created by the hopper-shape element at the leg outlet and lead to the load interaction between flow and leg body.

The variation of the average velocity of flow at the leg outlet is illustrated in Fig. 16. The following relation gives the rate of kinetic energy at the leg outlet.

$$\dot{K} = \frac{1}{2}\dot{m}v^2 \qquad \text{Eq.(8)}$$

For the present case, with the average values of flow rate (100kg/s) and outlet velocity (1.6 m/s), $\dot{K} = 128\,J/s$ whereas, the initial rate of gravitational potential energy at the inlet of the leg is

$$\dot{U} = \dot{m}gh \qquad \text{Eq.(9)}$$

It is about 6867 J/s for the present values of flow rate and leg height. The difference between these two values is due to the rate of work of friction force from the leg body to the material flow. The average friction force can be estimated by the following relation:

$$F = \frac{\dot{U}-\dot{K}}{V} = 4.21\ kN \qquad \text{Eq.(10)}$$

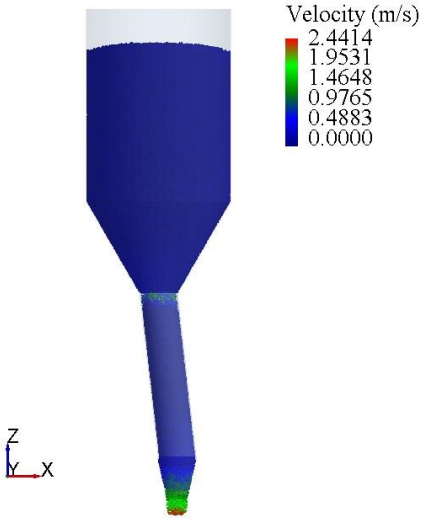

Fig. 13. Contour of material velocity at t=10s.

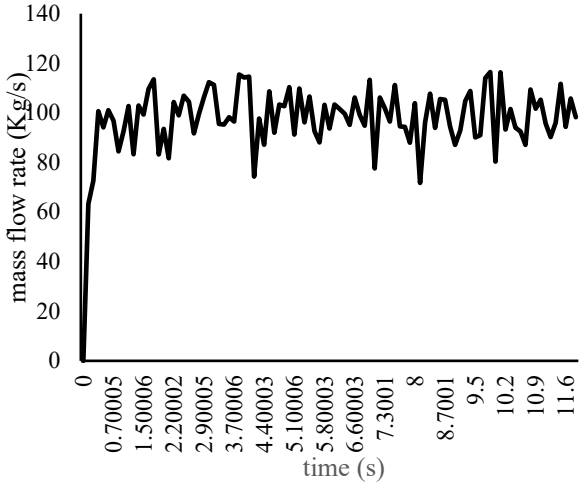

Fig. 14. Variation of material flow rate versus the simulation time.

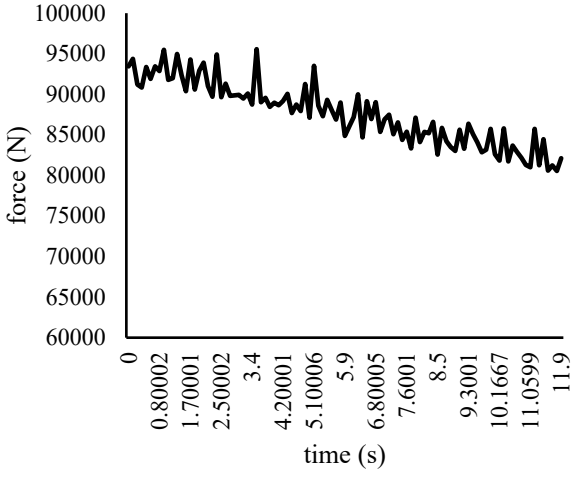

Fig. 15. Variation of load interaction between flow and leg body versus simulation time in case2.

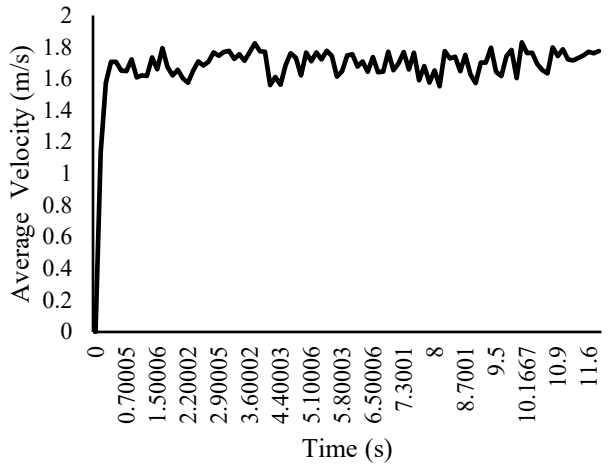

Fig. 16. Variation of the average flow velocity at the leg outlet.

8. Results and Discussion

Data collection is the most important way to a better understanding of mechanical events. Here, the data collection revealed, against the misunderstanding viewpoint, that the leg vibration occurrence is independent of the shocks in the other elements such as the furnace and the product cooler. The data of Fig. 4. and the subsequent explanations told this. The next relations (Eq.1) and evaluations (Fig. 7.) determined that the leg vibration is a type of free vibration that is initiated by an unknown external excitation. The damping parameters illustrated (Fig. 8.) that the vibration cannot last more than a few seconds without the external excitation and this clarified the existence of a continuous excitation. The material motion in the leg pipe was determined as the most important candidate for the excitation. DEM simulations (Fig. 15.) confirmed the variable form of the contact force which matched with the external excitation.

9. Conclusions

Data collection revealed that there are some cases in which the leg vibration initiation does not match with the shocks in the product cooler. Further investigations revealed that these shocks are indirectly the reason for the leg vibration by opening the leg outlet and leading to the material flow. Interaction between the flow and leg body acts as an actuation load for the leg vibration. The vibration-related parameters of the leg were discussed to be possibly determined exactly or be estimated approximately. Results showed that the evaluated natural frequency was close to the measured frequency which confirmed that the vibration of the leg has a free vibration nature which is actuated by the random external excitation sourced from the material flow. According to the known parameters, a relation was derived between the force and the natural frequency ratio which gave an estimation of the value of the actuating force as a function of frequency. The DEM simulations gave the results that confirmed the findings of the present work.

Acknowledgment

The authors would like to thank the GISDCO deputy of development and engineering for their scientific, economic, and spiritual support in conducting the present research.

References

[1] Atsushi M, Uemura H, Sakaguchi T, MIDREX processes, Kobelco Technol Rev. 2010; 29: 50–7.
[2] Hamadeh H, Mirgaux O, Patisson F, Detailed modeling of the direct reduction of iron ore in a shaft furnace, Materials. 2018; 11(10): 1865.
[3] Valipour M.S, Saboohi Y, Numerical investigation of non-isothermal reduction of hematite using syngas: the shaft scale study, Model Simul Mater Sci Eng. 2007; 15(5): 487.
[4] Boechat F.O, de Carvalho R.M, Tavares L.M, Simulation of mechanical degradation of iron ore pellets in a direct reduction furnace. KONA Powder Part J. 2018; 35: 216–25.
[5] Hosseini A, Faghih Khorasani A, Experimental and numerical study of the rib effect in a gas-gas heat exchanger performance used in a sponge iron production plant (MIDREX), Proc Inst Mech Eng Part A J Power Energy. 2021; 09576509211007969.
[6] Munro W.D, Amundson N.R, Solid-fluid heat exchange in moving beds, Ind Eng Chem. 1950; 42(8): 1481–8.
[7] Amundson N.R, Solid-fluid interactions in fixed and moving beds with small particles, Ind Eng Chem. 1956; 48(1): 26–35.
[8] Siegmund C.W, Munro W.D, Amundson N.R, Two problems on moving beds. Ind Eng Chem. 1956; 48(1): 43–50.
[9] Shams A, Moazeni F, Modeling and simulation of the MIDREX shaft furnace: reduction, transition and cooling zones, JOM. 2015; 67(11): 2681–9.